Hindawi
International Transactions on Electrical Energy Systems
Volume 2022, Article ID 7894264, 14 pages
https://doi.org/10.1155/2022/7894264

Research Article

An Efficient Design of Adaptive Model Predictive Controller for Load Frequency Control in Hybrid Power System

Muhammad Majid Gulzar,[1] **Daud Sibtain**,[1] **Arslan Ahmad**,[2] **Imran Javed**,[3] **Sadia Murawwat**,[4] **Imran Rasool**,[1] **and Aamir Hayat**[1]

[1]*Department of Electrical Engineering, University of Central Punjab, Lahore, Pakistan*
[2]*Otto von Guericke University Magdeburg, Magdeburg, Germany*
[3]*Department of Electrical Engineering, University of Engineering and Technology Lahore, Narowal Campus, Narowal, Pakistan*
[4]*Department of Electrical Engineering, Lahore College for Women University, Lahore, Pakistan*

Correspondence should be addressed to Daud Sibtain; daudsibtain@gmail.com

Received 20 December 2021; Revised 25 February 2022; Accepted 28 February 2022; Published 18 April 2022

Academic Editor: Pawan Sharma

The technology has proceeded so much that the power system should be substantial and explicit to give optimal results. Ever-increasing complexities of the power system and load disparity cause frequency fluctuations leading to efficiency degradation of the power system. In order to give a suitable real power output, the system entails an extremely perceptive control technique. Consequently, an advanced control method, that is, an adaptive model predictive controller (AMPC), is suggested for load frequency control (LFC) of the series power system which comprises photovoltaic (PV), wind, and thermal power. The suggested method is considered to enhance the power system execution as well as to decrease the oscillations due to a discrepancy in the system parameters and load disturbance under a multi-area power system network. The AMPC design verifies the constant frequency by maintaining a minimum steady state error under varying load conditions. The proposed control approach pledge that the steady-state error of frequencies and interchange of tie line powers is maintained in a given tolerance constraint. The effectiveness of the proposed controller is scrutinized by conventional controllers like genetic algorithm-tuned PI (GA-PI), firefly algorithm-tuned PI (FA-PI), and model predictive controller (MPC) to show the competence of the proposed method.

1. Introduction

1.1. Literature Review. In the past decade, conventional energy resources were utilized to fulfill the demand of energy requirements. Unfortunately, the natural energy resources like coal, gas, oil, and so on are decreasing and there is a critical need for some other measures to compete with the necessity of increasing energy demands. This substantial situation induces the use of renewable resources, for instance PV, wind, hydro, and so on, which became the popular topic of research during the past few years. As renewable resources play an indispensable role in attaining the goal of energy demand, around 18% of energy need is currently being satisfied through these resources worldwide [1]. Renewable resources are sustainable and will never run out. These energy resources require less maintenance, and their cost of operation is also reduced because they depend on natural and available resources like sun, wind, heat, and so on. Renewable resources produce one-fifth of the world's electric power in accordance with the Renewables Global Status Report (GSR) [2].

The concatenation of nonconventional sources with conventional sources is complex. In order to meet certain requirements of current and voltage for the balanced power system, different techniques are adopted in the renewable resources to minimize the disturbances caused by them during grid connection [3]. Controlling the frequency deviation within a specified limit is necessary for the operation

of a balanced power system, and for these, different techniques and controllers have been used. The penetration of renewable energy resources into grid power systems causes frequency deterioration. Many factors like load perturbation, faults, expeditious change in load and operational unreliability, and so on deteriorate the implementation of the electrical power system [4].

Power grids are composed of a number of different interconnected areas that are connected to each other via a transmission line (tie line). In a single area, thermal generator is usually affixed to a set of renewable energy sources to satisfy its own energy requirements and control power switching within adjoining areas. However, the changes occurring in the generation and load side lead to the deviation of voltage and frequency from its limits [5]. The infusion of renewable resources in this research article consists of solar PV, wind turbine, and thermal energy generators.

PV system is rapidly growing technology and is the most abundant renewable source due to its numerous advantages like no release of harmful air, eco-friendly, and locally available renewable resources [6, 7]. The incorporation of renewable energy into the power grid gives rise to perturbation in system frequency. The speed of wind is wavering for the whole year in particular places which results in the disparity of output power and frequency of wind generators. The photovoltaic output is dependent upon the climatic condition that varies with the change of climate. So, it is hard to manage the frequency of the hybrid generating system without any latest control method because of the unpredictable nature of renewable sources. The grid power may be affected by the outcome of renewable energy sources, thus originating a serious issue from the frequency deviation of the grid. Also, an unexpected change of load demands precipitates for power imbalance and frequency fluctuations. The two-area PV-wind connected thermal grid system is depicted in Figure 1.

A reliable and working power system should be balanced irrespective of inconsistent load and system disruption. In wind power generation under uncertainty of load requirements and arbitrary input of wind power, the pitch controller will no longer be able to control the frequency of the system constructively due to their inactive response [8]. Therefore, it is essential that the power system frequency is unchanged during any discrepancy in the load demand. That is why the significance of LFC in the design and working of the electric power system has come into consideration. The core function of LFC is to regulate the frequency of each area within limits and to make the flow of the tie line power suitable during the changing load requirements [9]. To counter the challenge of LFC various control methods are studied, like modern or advanced approach with linearity and nonlinearity approaches are analyzed [9].

To counter the challenge of LFC, various control methods are studied, like modern or advanced approach with linearity and nonlinearity approaches are analyzed [10,11]. LFC plays a very important role in the working and designing of a system. Due to uncertain and unpredictable changes in load, the system frequency gets

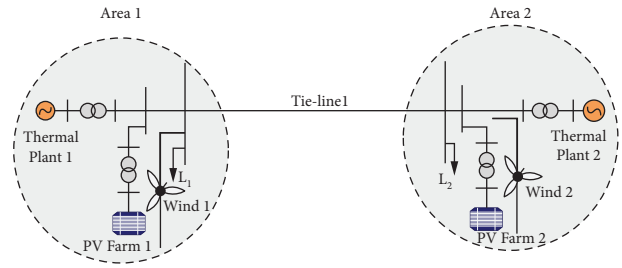

Figure 1: Two-area hybrid grid connected system.

affected which is not required. However, by using the LFC method either by escalating the capacity of generation or by reducing the frequency fluctuations, this problem can be resolved by keeping the values within certain limits. This phenomenon is known as load frequency control [12]. An appropriately working power system should resist the load perturbation and must provide productive power quality by maintaining both frequency fluctuation and production capacity within normal limits. Research work, for instance [13, 14], shows fundamental information about different frequency regulations of an interconnected power system. Because of the complication of the modern power system, these frequency oscillations when open to any unwanted interference may expand to a wide interlinked system of the various control area. It originates unwanted interference that causes uncertainty which will result in the blackout of the complete power system [15–17].

Different controllers are proposed in the literature to mitigate LFC problems, such as artificial neural network (ANN) [18], hybrid artificial neural network [19] to track maximum power point tracking, fuzzy approach [20], cascade fuzzy-proportional integral derivative incorporating filter (PIDN)-fractional order PIDN (FPIDN-FOPIDN) [21], and wavelet neural network with data filtering [22] to escalate the execution of LFC methodology. Classical control techniques are used to overcome the LFC issue. In [23], a proportional integral (PI) controller and dual-mode PI controller were used for the design of frequency changing problems with communication delays, and it also discussed the hydropower system with the use of PI control. PI with MPC was used in [24] to attain better closed-loop results. Similarly, a lot of work was carried out with integral derivative (ID), and the cascaded design was proposed in [25], where (1 + PD)-PID was formulated to counter frequency oscillation under uncertain conditions. Similarly, cascade-fractional order ID with filter ($C - I^{\lambda}D^{\mu}N$) was proposed in [26]. In [27], the authors highlighted the idea about scheduling the integral gains using GA-based fuzzy control algorithm. In [28], fuzzy logic-based LFC regarding high penetration of wind turbines was presented. In [29], sliding mode control (SMC) was proposed, JAYA optimization was proposed in [30], and a PSO-based sliding mode controller was discussed in [31]. In [32], a MPC-based PV connected thermal two-area system was presented for the LFC problem. Similarly, in [33], a MPC-based thermal-thermal connected system for the LFC problem was presented. The flowchart of the survey conducted on LFC depending on the controller and area is shown in Figure 2.

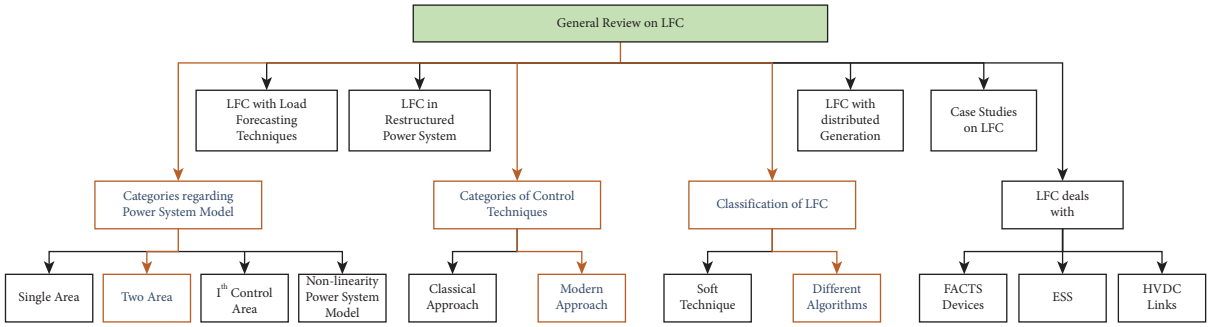

Figure 2: Review on LFC.

Figure 2 presents the fundamental execution of various power system models and includes the load forecasting technique in LFC. Here, the classification of LFC is studied like soft technique and other various algorithms. Moreover, it also illustrates the application of different FACTS devices, energy storage systems (ESSs), and HVDC links incorporation with LFC [13].

1.2. Research Gap and Motivation. After considering the detailed literature, the survey has identified void sections that need to be dealt with the proposed methodology. The research gap and motivation are as follows:

(i) The literature survey sheds light on the studies performed by the researchers in the field of LFC, and they have presented exclusive ideas to deal with frequency in order to maintain stable operation of the power system under the load disturbance.

(ii) An advanced controller in the form of adaptive model predictive controller (AMPC) is proposed for multi-area sets to be a unique control technique having the ability to counter under uncertainty and controlling attenuation due to external disturbance.

1.3. Contribution and Paper Organization. The motivation has paved the way towards the following contributions and novelties:

(i) In this paper, the multi-area PV, wind connected thermal systems are developed, where the importance of penetration level of renewable sources and its impacts on the system has been kept in consideration during designing.

(ii) Designing of the PV, wind, and thermal system is carried out where doubly fed induction generator (DFIG)-based wind turbine model is designed, where the pitch actuator is controlled by MPC.

(iii) Adaptive model predictive controller (AMPC) is presented to control the LFC problem in a multi-area power system to mitigate frequency fluctuations.

(iv) AMPC is designed in such a manner that it fulfills two requirements ensuring the LFC requirement under uncertainty and controlling attenuation due to external disturbance. The scaling factor is introduced in the output which is adjusted in each sampling time by an adaptive mechanism.

This paper is organized as follows. Section 2 establishes the system modeling of PV, wind, and thermal power systems. Section 3 represents the overall model of a hybrid power system. In Section 4, the controller based on AMPC is proposed. Section 5 is regarding the simulations and results analysis of the proposed controller. Finally, Section 6 concludes the paper.

2. Thermal Generator Prototype

The thermal generator prototype comprises a generator, governor, reheater, steam turbine, and droop. Governor is utilized to handle the speed of the turbine that is based on the error, which is the difference of power and frequency ($\Delta P - \Delta f$). Moreover, the governor manages the mechanical motion of the turbine by supervising the working of the valve and by recovering the lost energy subsequently going through reheater, which supports to attain the mandatory goal. The speed of prime mover is controlled with the help of droop, which is attached to the generator. The generator is the last unit in the thermal power system, which transforms the mechanical motion into electricity, which is our fundamental demand [34]. The thermal power plant is modeled for the capacity of 4000 MW operating at 2200 MW at 50 HZ. The speed governor equation has two inputs, the reference power ΔP_{ref} and change in frequency Δf and governor output $\Delta P_g(s)$ is given by:

$$\Delta P_g(s) = \Delta P_{\text{ref}}(s) - \frac{1}{R}\Delta f(s), \tag{1}$$

where $(1/R)$ represents the droop which acts like a valve to control the flow.

Furthermore, in the two-area case, a bias factor is interconnected with a tie line, which specifies the quantity of power transferred within two areas which is described in the following equation:

$$\Delta P_{ij} = T_{ij}\left(\Delta f_i - \Delta f_j\right), \quad i \neq j. \tag{2}$$

For the ith area, the area central error (ACE) and tie line power variation are stated as

$$ACE_i = B_i \Delta f_i + \Delta Tie_{ij}, \quad i \neq j, \tag{3}$$

where B_i is the frequency bias factor parameter.

The output of the generator is Δf_i which has two inputs $\Delta P_R(s)$ and $\Delta P_d(s)$, where $\Delta P_d(s)$ is the load disturbance in the system and the output Δf_i is given in the following equation:

$$\Delta f_i(s) = G_p(s)\left[\sum_{j=1}^{n} \Delta P_{Rij} - \Delta P_{d,i} - \Delta P_{tie,i}\right], \tag{4}$$

where $G_p(s) = 1/(M_i s + D_i)$, and output of the generator is dependent upon the disturbance in the load. The generator will always adjust its output power to meet the power demand.

3. Photovoltaic Prototype

The most extensively utilized renewable source of energy is the PV system. The current source is in parallel with the diode, making it a nonlinear current source, which exactly transforms the solar irradiation into electricity by propagating the movement of electrons and holes within the PV cell. As it is a nonlinear current source, it is necessary to form the PV source to inevitably work on its MPPT so that maximum power can be achieved [35].

Figure 3 demonstrates the I-V curve attributes at 25°C. As irradiance reduces from 1000 (W/m^2) to 200 (W/m^2), I_{pv} also reduces correspondingly. At 500 (W/m^2), the current value is half of its max value, and there is a slight effect on voltage V_{pv}. In this paper, the PV for the integrated system is reviewed to work at MPPT, at 1000 (W/m^2) at 25°C. PV system is designed for 150 to 30 kW connect with a constant voltage source of 6 kV at PV array side with penetration level set to 40 percent.

Integrating PV array with a thermal power system needs to go through various steps to get interconnected. The designing of PV system composed of various parts like converter, inverter, and calculation of average power actually fed to the grid as shown in Figure 4.

Here, the designing of the PV system is carried out. AC voltage can be estimated using

$$q = \frac{v_{dc}}{v_{ac}}, \tag{5}$$

where q is the gain between AC and DC voltage in the system and its value is generally less than 0.86. For this prototype, its value is 0.7.

The transfer function of the boost converter can be estimated by using equations (6) and (7).

$$m_1 = \frac{v_2}{v_1} = \frac{i_1}{i_2}, \tag{6}$$

$$g_1(s) = \frac{1}{m_1}, \tag{7}$$

where $(1/m_1)$ is the gain of the boost converter. The transfer function of the inverter is mentioned in the following equation:

$$g_2(s) = \frac{I_{ac}(s)}{I_2(s)} = \frac{s^2}{s^2 + \omega^2}, \tag{8}$$

where $\omega = 2\pi f = 2\pi(50) = 314.12$ rad/sec. For instantaneous power, the transfer function is given in the following equation, where (v_m/i_m) is the impedance.

$$P(s) = \frac{v_m i_m}{2s} + \frac{v_m i_m}{2} \frac{s}{s^2 + (2\omega)^2}. \tag{9}$$

The gain in instantaneous power is mentioned in the following equation:

$$g_3(s) = \frac{p(s)}{I_{ac}(s)} = v_m \left(\frac{\left(s^2 + \omega^2\right)\left(s^2 + (2\omega)^2\right)}{s^2\left(s^2 + (4\omega)^2\right)} \right). \tag{10}$$

The Laplace domain equation for average power is given in the following equation:

$$p_{avg}(s) = \frac{v_m i_m}{2s}. \tag{11}$$

The gain for average power is described in the following equation:

$$g_4(s) = \frac{p_{\text{avg}}(s)}{p(s)}. \tag{12}$$

3.1. Wind System. The contribution of wind energy in the power system is the main concern. Wind energy variation urges auxiliary power imbalance to the power system and causes frequency fluctuations from its nominal value. Owing to this fact, the interconnection of wind into the power system causes LFC problem [36, 37]. To deal with the LFC problem, an optimum controller is needed which addresses the increasing complexity of the power system and the involvement of renewable resources into the power system. This paper introduces a decentralized AMPC to resolve the LFC problem, and this controller will show its superiority as compared to other controllers.

3.2. Modeling for a Single Wind Turbine. The wind power system is divided into two main sections: (1) electrical and (2) mechanical. The electrical system consists of an MPPT calculator, which calculates the maximum power based on ω. Furthermore, it also contains the inverter which generates the reference power, according to which output power is generated and here the generator converts mechanical power into electrical power and then feds it to the grid, and overall, the wind system is designed at 150 kW rating. The mechanical portion consists of a rotor speed controller which senses the power and torque of the turbine. On the basis of these factors, it gives feedback to the pitch controller which controls the pitch actuator angle to control the orientation of the wind turbine. The overall wind model is shown in Figure 5.

To carry out the modeling of the wind system for the LFC problem, the state-space equation is formulated and designing of each part of the wind model is carried out.

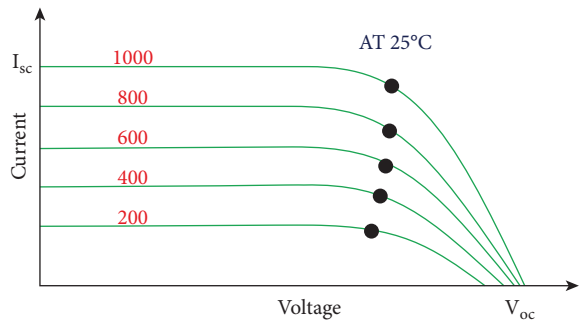

Figure 3: PV characteristics.

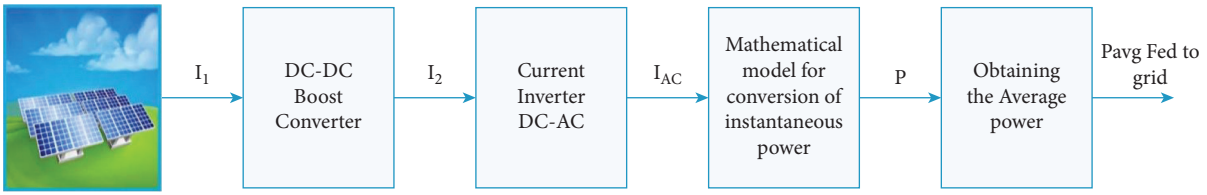

Figure 4: PV farm connected grid prototype.

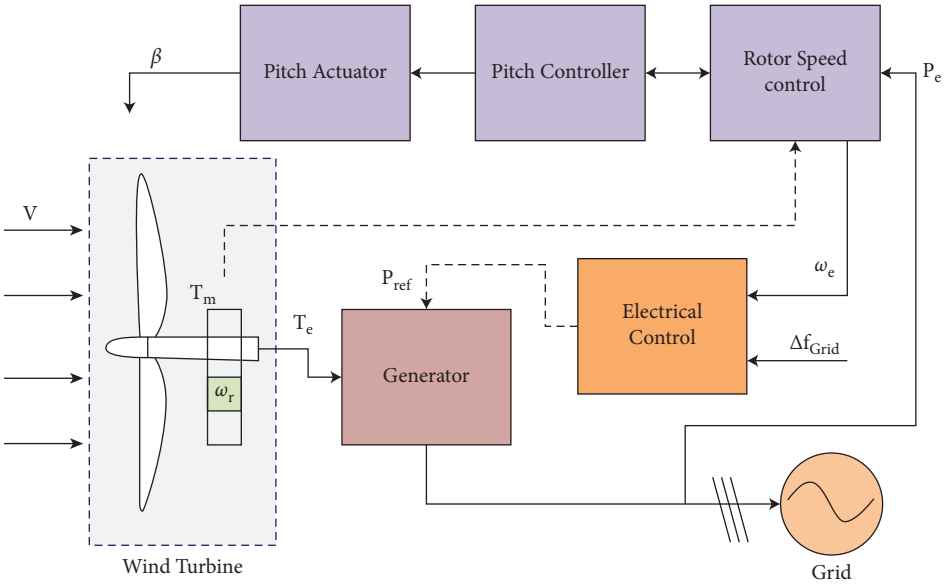

Figure 5: Block diagram of LFC DFIG-based wind farm.

Rotation of wind turbine is given by wind power P_w represented by

$$P_w = \frac{1}{2}\rho A V_w^3, \tag{13}$$

where ρ represents air density, cross-sectional area is represented by A, and wind speed is represented by V_m.

The aerodynamics of the wind turbine allow to absorb mechanical power P_m which is expressed as cube of wind speed.

$$P_m = C_p(\lambda, \beta) P_w. \tag{14}$$

Further, it can be elaborated under per unit value system.

$$P_m = \frac{C_p}{C_{p-n}} \left(\frac{V}{V_n}\right)^3, \tag{15}$$

where C_p is related to λ (TSR) and β represents the pitch angle of the turbine. For calculation of C_p, the simplified formula is introduced as [38]

$$\Delta\lambda = \frac{\lambda_n V_n}{w_{r-n} V_\circ} \Delta w_r, \tag{16}$$

where $w_{r-n} = 1.2$ pu from a case study.

From equation (16), ΔC_p can be modified as

$$\Delta C_p = \frac{\partial C_p}{\partial \omega_r}\Delta\omega_r + \frac{\partial C_p}{\partial \beta}\Delta\beta. \tag{17}$$

So, to rewrite P_m, ΔP_m can be written as

$$\Delta P_m = X_\omega\left(\frac{\partial C_p}{\partial \omega_r}\Delta\omega_r + \frac{\partial C_p}{\partial \beta}\Delta\beta\right), \tag{18}$$

where $X_\omega = V_\circ^3/(C_{p-n}V_n^3)$.

The following condition can be addressed here; if $\beta = 0$, rated speed equation (18) becomes

$$\Delta P_m = X_\omega\frac{\partial C_p}{\partial \omega_r}\Delta\omega_r. \tag{19}$$

If $\beta > 0$ above rated speed, the pitch angle is changed for capturing wind power. The diagram for the pitch angle is shown in Figure 4. ΔP_m is represented as

$$\Delta P_m = X_\omega\left[\left(\frac{\partial C_p}{\partial \omega_r}\Delta\omega_r + K_p\frac{\partial C_p}{\partial \beta}\right)\Delta\omega_r + K_i\frac{\partial C_p}{\partial \beta}\Delta\theta\right]. \tag{20}$$

The origination of equation (20) takes place by describing the pitch angle as

$$\Delta\beta = K_p\Delta\omega_r + K_i\Delta\theta, \tag{21}$$

where K_p and K_i are gains of the PI controller to change the angle $(\mathrm{d}\theta/\mathrm{d}t) = \Delta\omega_r$.

Furthermore, considering the importance of the gearbox, designing of maximum power tracking calculation is carried out for rotational speed [39].

$$\omega_r = \frac{1}{2H_\omega s + F}\left(T_m - T_e\right), \tag{22}$$

where $T_m = (P_m/\omega_r)$ and $T_e = (P_e/\omega_r)$ and the above equation can be modified for the above-rated speed as

$$\begin{aligned}\frac{\mathrm{d}\Delta\omega_r}{\mathrm{d}t} &= \frac{X_\omega\left(\left(\partial C_p/\partial\omega_r\right) + K_p\left(\partial C_p/\partial\beta\right)\right) - F\omega_{r\circ}}{2H_\omega\omega_{r\circ}}\Delta\omega_r - \frac{1}{2H_\omega\omega_{r\circ}}\Delta P_e + \frac{X_\omega K_i\left(\partial C_p/\partial\beta\right)}{2H_\omega\omega_{r\circ}}\Delta\theta,\\ P_{\omega r} &= X_c\left(\frac{\omega_r}{\omega_{r-n}}\right)^3.\end{aligned} \tag{23}$$

During the LFC process, $\Delta P_{\omega r}$ can be calculated as

$$\Delta P_{\omega r} = \frac{3X_c}{\omega_{r-n}^3}\omega_{r\circ}^2\Delta\omega_r\theta. \tag{24}$$

Another section is a generator from [40]; the transfer function for first-order active power control for wind form is determined by the response time of generator current control, which can be written as

$$P_e = \frac{1}{\tau_e s + 1}P_{\mathrm{ref}}, \tag{25}$$

where $P_{\mathrm{ref}} = P_{\omega r} + P_f$.

Change in electrical power can be written as

$$\frac{\partial\Delta P_e}{\partial t} = \frac{1}{\tau_e}\left(-\Delta P_e + \Delta P_{\omega r} + \Delta P_{\omega f}\right). \tag{26}$$

The above presented equations for the model of wind system can be compiled into a state-space model for the above-rated wind speed, and it can be written as

$$\begin{cases}\dot{X} = Ax + Bu,\\ y = Cx + Du.\end{cases} \tag{27}$$

The generating matrix for A, B, and C is as follows:

$$A = \begin{bmatrix}\dfrac{X_\omega\left(\left(\partial C_p/\partial\omega_r\right) + K_p\left(\partial C_p/\partial\beta\right)\right) - F\omega_{r\circ}}{2H_\omega\omega_{r\circ}} & X_\omega K_i\dfrac{\left(\partial C_p/\partial\beta\right)}{2H_\omega\omega_{r\circ}} & -\dfrac{1}{2H_\omega\omega_{r\circ}}\\ 1 & 0 & 0\\ \dfrac{3K_c\omega_{r\circ}^2}{\tau_e\omega_{r-n}^3} & 0 & \dfrac{-1}{\tau_e}\end{bmatrix}, \tag{28}$$

$$B = \begin{bmatrix}0 & 0 & \dfrac{1}{\tau_e}\end{bmatrix}^T, \tag{29}$$

$$C = \begin{bmatrix}0 & 0 & 1\end{bmatrix}. \tag{30}$$

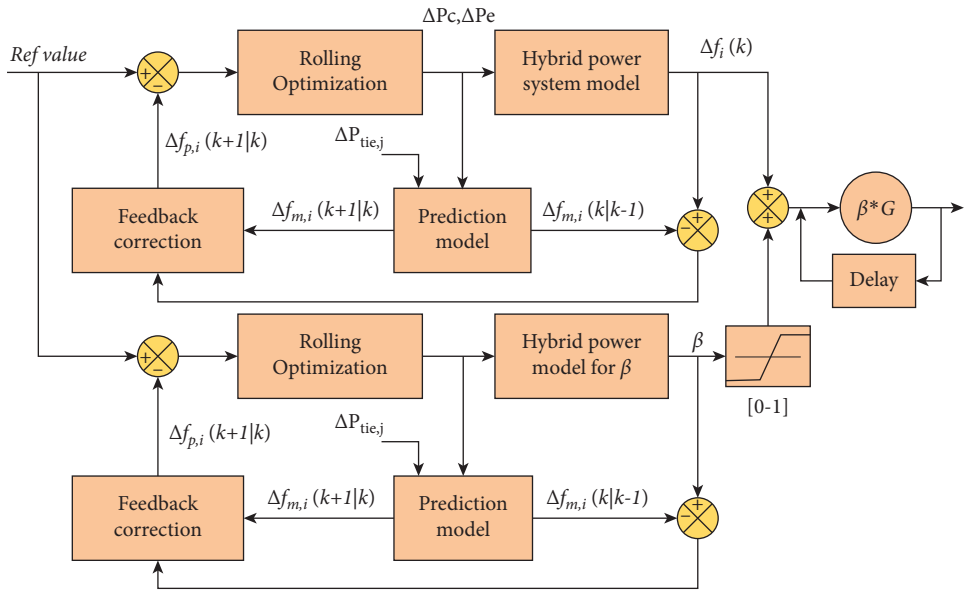

Figure 6: The block diagram for AMPC strategy.

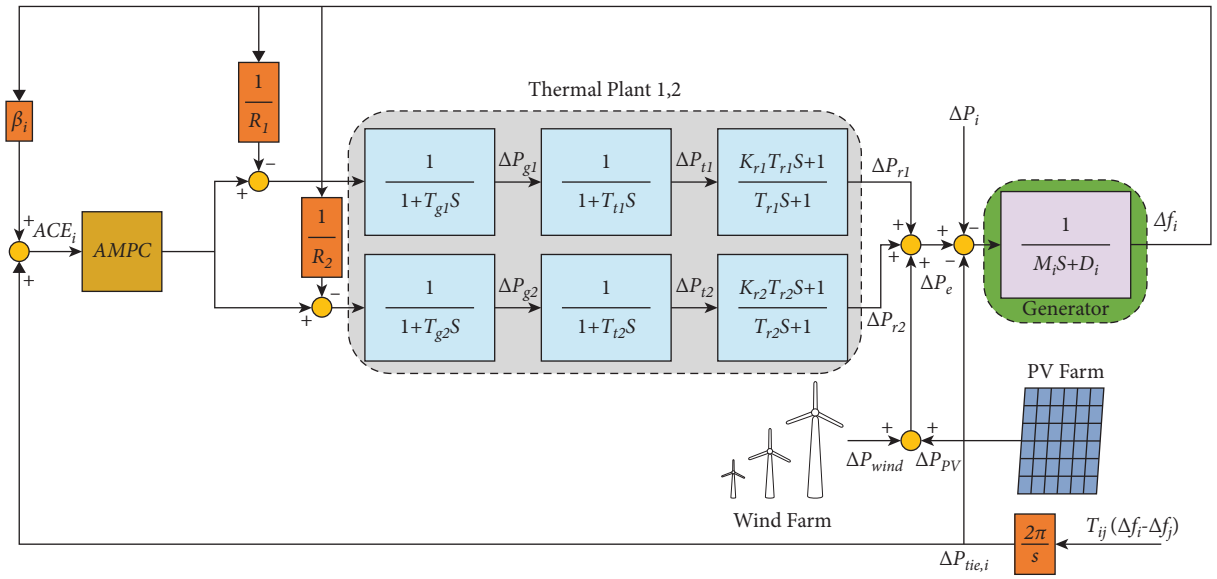

Figure 7: Two-area hybrid interconnected thermal system.

4. Adaptive Model Predictive Controller

MPC is an advanced control algorithm used in many industries to resolve the industrial process to satisfy a number of constraints to deal with linear and nonlinear problems. It was first proposed by Richalet in 1978 [41]. This MPC has a great potential in dealing with the system having disturbance and also dealing with optimization requirements of the system. MPC mainly contains three blocks: rolling optimization, prediction model, and feedback correction. The rolling optimization block is used to optimize a number of constraints online which differentiate it from traditional optimal control. The next part is the prediction model which predicts the future value in real time, and this model is basically working on the history of the controlled object. Moreover, it is designed for multi-input/output constraints. The last block is the feedback correction which is actually calculating the deviation from the predicted value and the actual output value [42].

As from its name, it is obvious that feedback correction compensates the future error while utilizing the feedback information to develop the closed-loop optimization operation. This paper presents an adaptive model predictive controller (AMPC). This controller is designed to deal with the constraints of the LFC problem. AMPC is presented in Figure 6.

The designing of this controller is established in such a way that the one section is dealing with the LFC requirements in presence of uncertainty $\Delta F_i\ (k)$. The other part of MPC is designed to deal with the attenuation effect due to

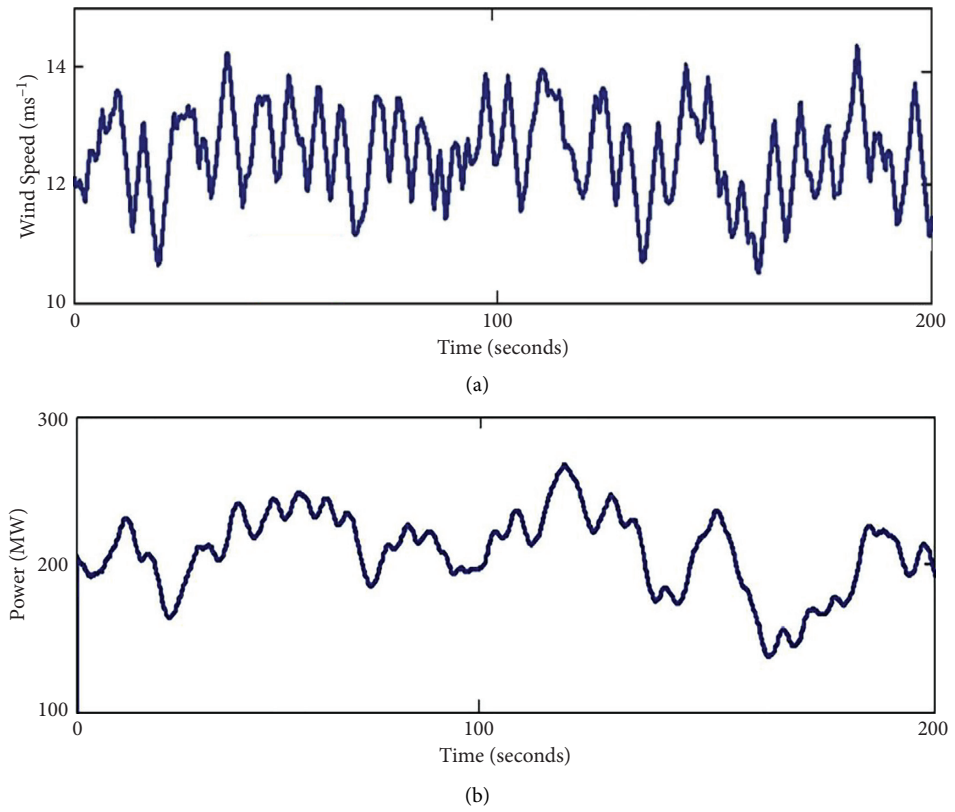

Figure 8: Wind speed and power: (a) wind speed; (b) wind power generation (MW).

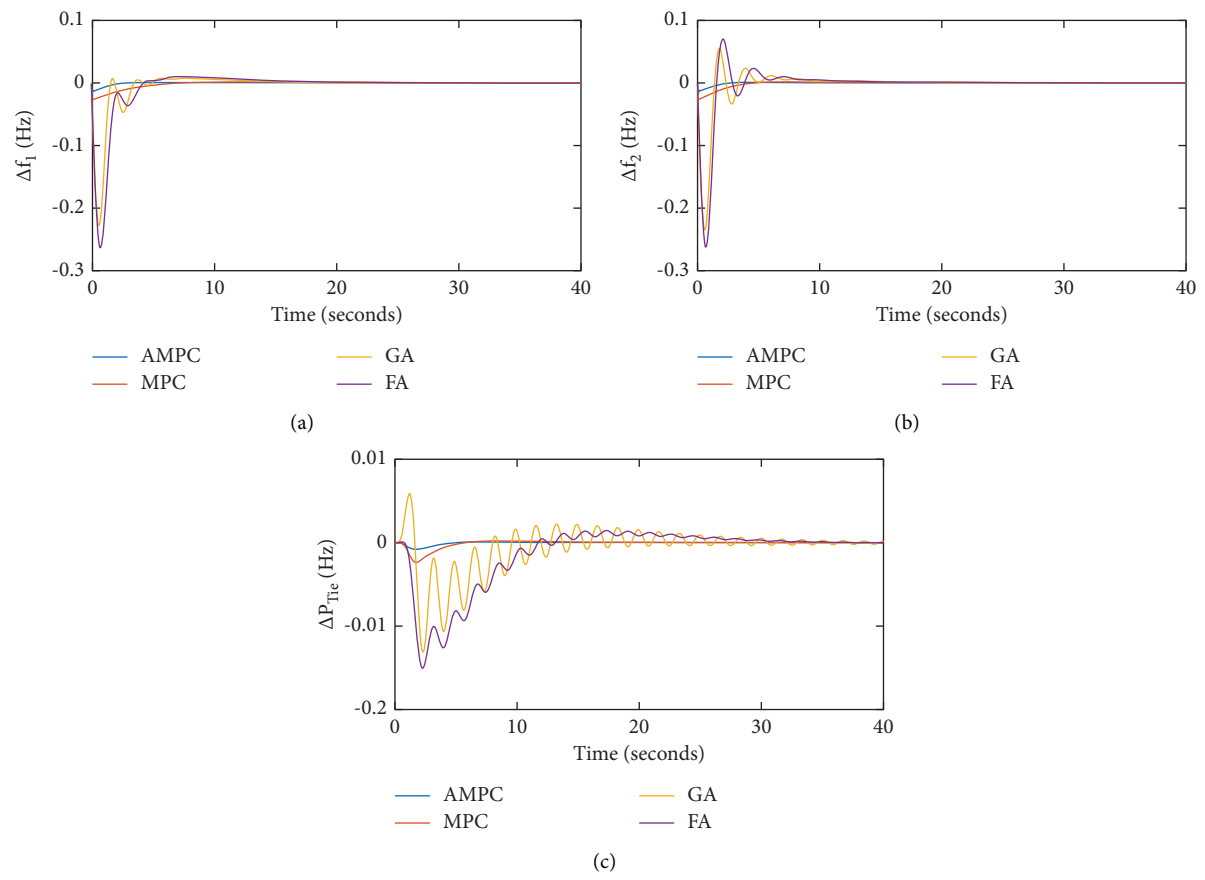

Figure 9: Frequency response and change in power: (a) Δf_1; (b) Δf_2; (c) ΔP_{Tie}.

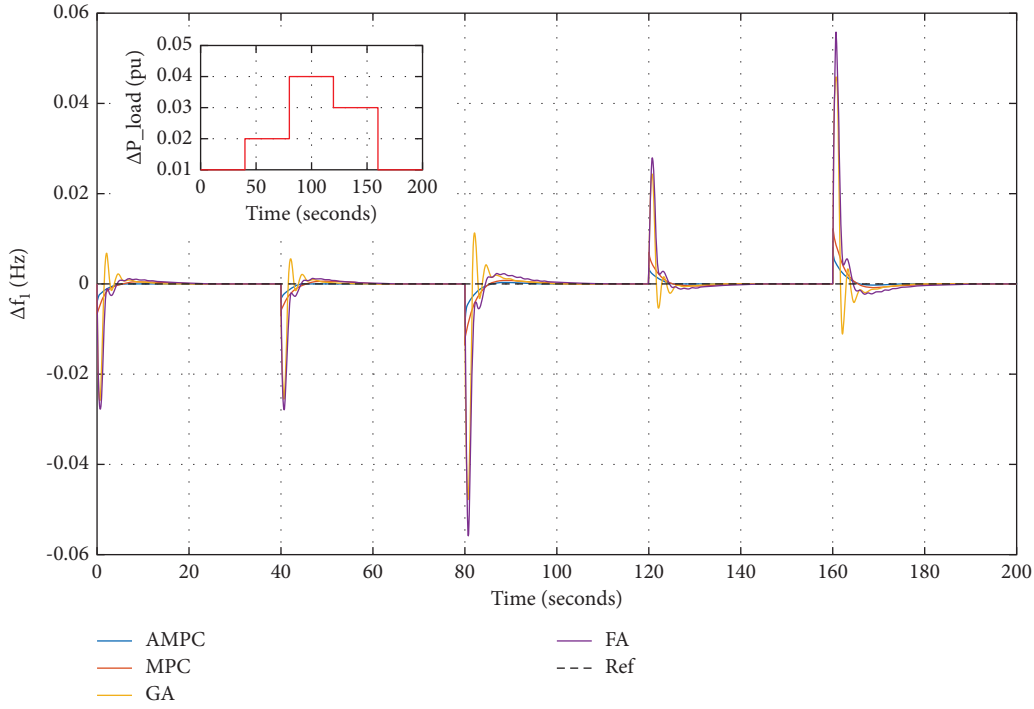

Figure 10: Controller response under varying load conditions for area 1.

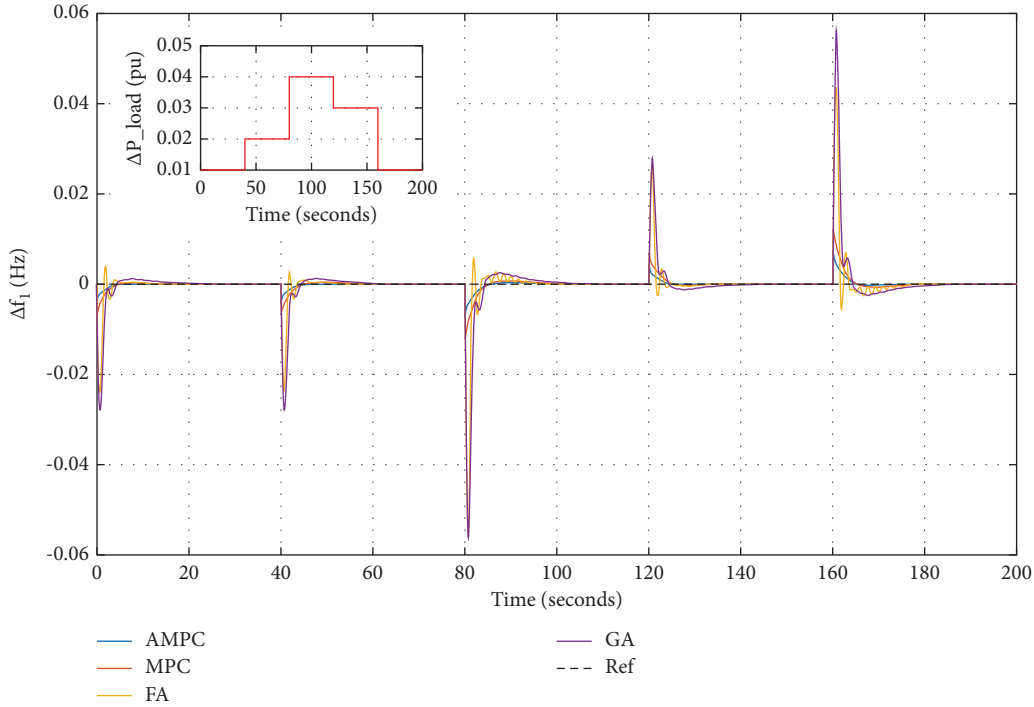

Figure 11: Controller response under varying load conditions for area 2.

external disturbance and to counter tie line variation. The other important element between the two areas is the frequency bias factor (β) whose value is between 0 and 1 and is used in balancing the ACE.. The last thing which is the output scaling factor (G) is set constant. The output scaling factor is adjusted in each sampling time by the adaptive mechanism.

4.1. Rolling Optimization. The designing of the controller is carried out in such a way to minimize the oscillation in the frequency due to disturbance in load. The controller should have the ability to restore the system frequency as quickly as possible to ensure the safe operation of the hybrid power system. The AMPC has the capability to show less oscillations with minimal undershoot and overshoot in frequency

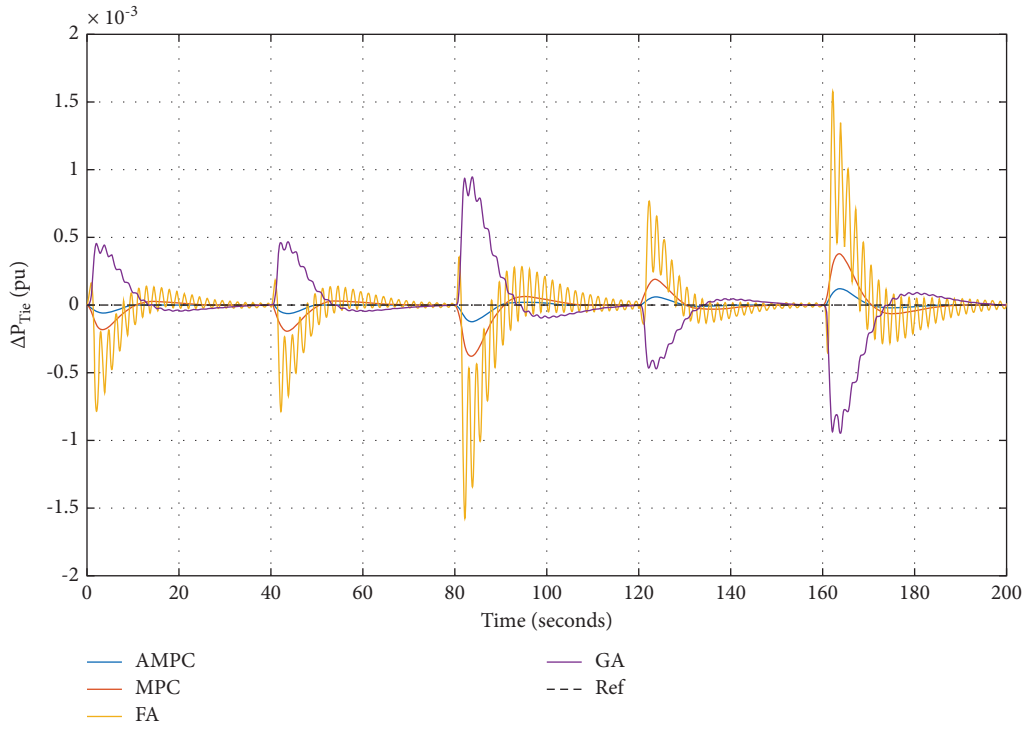

Figure 12: Exchange of power between two areas.

and prevent the violation of input and output constraints. The optimization is based on a steady-state model of the process, and it is typically a linear model used to minimize a profit function, minimizing cost function and maximizing production rate. The objective function is presented as follows.

$$J_i(k) = q_i\left[\Delta f_i(k+1)\right]^2 + r_{1,i}\left[\Delta P_{eb,i}(k)\right]^2 + r_{1,i}\left[\Delta P_{eu,i}(k)\right]^2. \tag{31}$$

Minimize the objective function. Min $J_i(k)$ for safe operation following constraints must be fulfilled.

$$\begin{cases} \Delta f_i^{\min}(k) \le \Delta f_i(k) \le \Delta f_i^{\max}(k), \\ \Delta P_{eb,i}^{\min}(k) \le \Delta P_{eb,i}(k) \le \Delta P_{eb,i}^{\max}(k), \\ \Delta P_{eu,i}^{\min}(k) \le \Delta P_{eu,i}(k) \le \Delta P_{eu,i}^{\max}(k), \\ 0 < \beta < 1. \end{cases} \tag{32}$$

Considering all these constraints in equation (32), the LFC efficiency is achieved and the transfer of active power is controlled accurately.

5. Results and Discussion

This section highlights the performance of the proposed model and control technique. The proposed technique is verified on MATLAB/Simulink. The two-area hybrid power system is proposed where the control of the PV, wind, and thermal power system is controlled by AMPC. Each area contains a set of PV, wind, and thermal power plant, and they are connected via a tie line as shown in Figure 7.

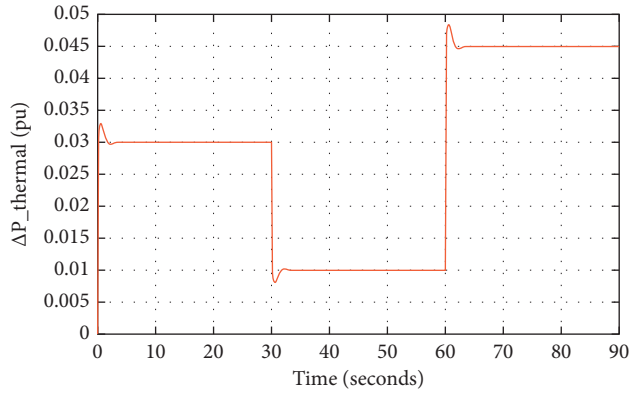

Figure 13: Thermal output power response.

The output generation of power by a wind turbine under varying wind conditions is presented in Figure 8. The control of the wind farm is carried out by MPC where the output pattern of power generation is obtained by applying varying wind patterns. The output generation of power is averaged around 200 MW, and wind speed varies between 9 and 14 ms^{-1}.

To verify the proposed technique, the two-area model is tested under different scenarios. Two different tests are applied to validate the efficiency of the proposed controller. (1) This step is applied for a step change in load at worst-case scenario that rarely occurs, and it is applied for both areas. (2) This step is very close to real-world scenarios, and the system load is varying throughout the day, so a varying test of load change is applied to monitor the performance of AMPC. Furthermore, the obtained results are compared

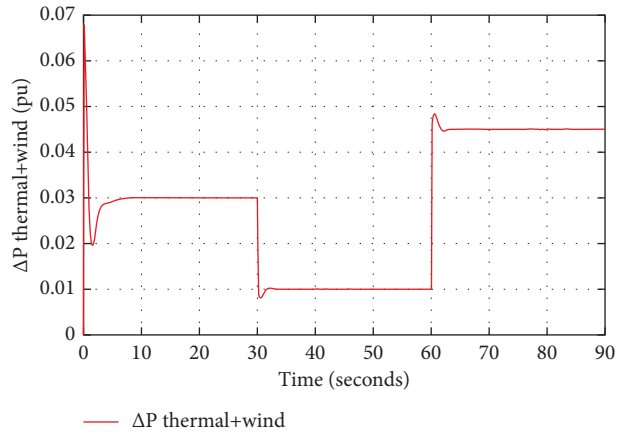

Figure 14: Thermal and wind power output response.

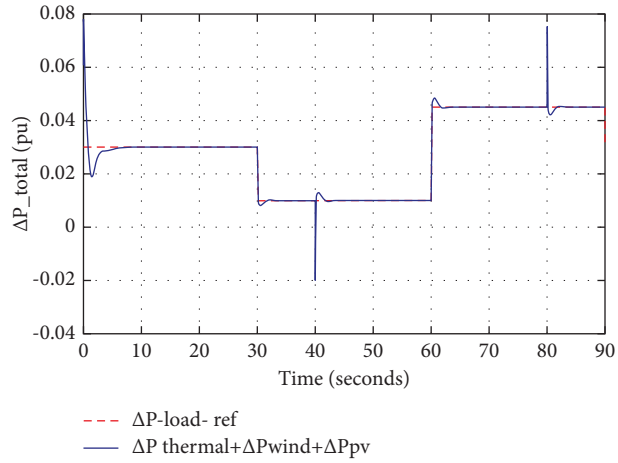

Figure 15: Collective power response of thermal, PV, and wind.

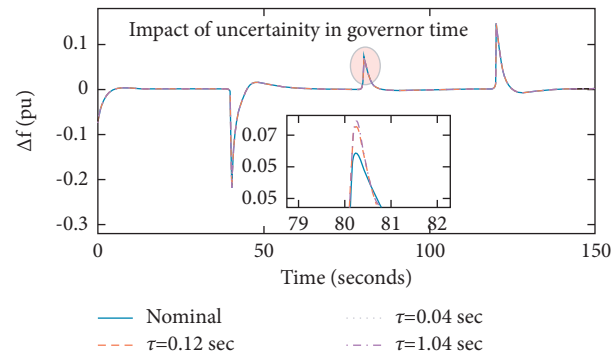

Figure 16: Response under uncertainty in the governor system.

with the state-of-the-art controllers. Figure 9 verifies the step response and the robustness of the proposed controller. In Figures 10 and 11, the validation for the varying load is monitored. The exchange of power between the two areas is also monitored as shown in Figure 12.

The power output response of thermal generator is shown in Figure 13, while the integration of wind with thermal is depicted in Figure 14. The collective response of thermal, PV, and wind is exhibited in Figure 15.

From the results, it is quite clear that AMPC is leading in superiority as compared to other controllers in terms of oscillation and response time which justify its robustness. Furthermore, the communication delay can originate in a system that is presented by time delay (τ),

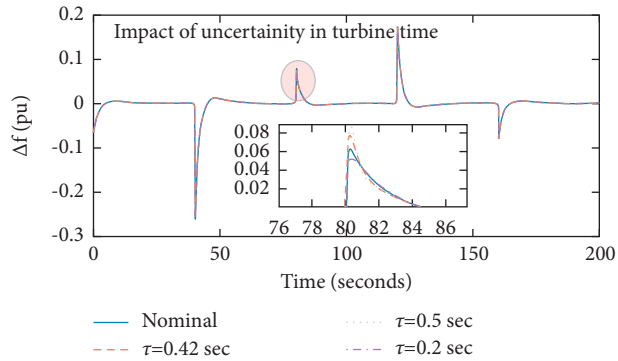

Figure 17: Response of controller under uncertainty in the turbine unit.

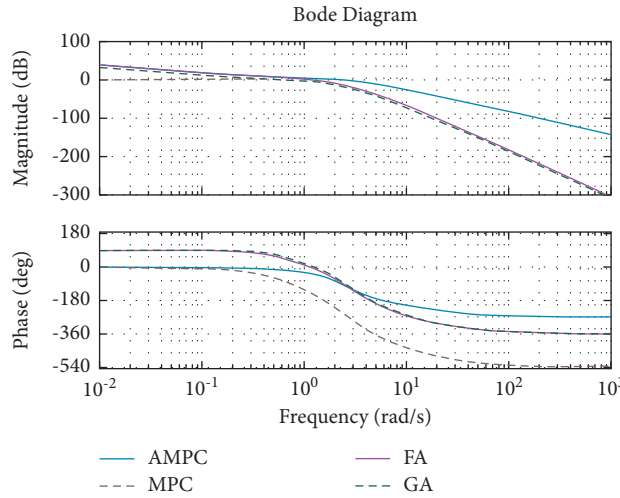

Figure 18: Stability response of controllers.

Table 1: Performance analysis of different controllers.

Controller	ITAE	ITSE	ISE
AMPC	0.1812	0.0001099	0.0001269
MPC	0.2012	0.0001348	0.0001721
GA	0.7908	0.001891	0.0009201
FA	0.8011	0.002004	0.0009316

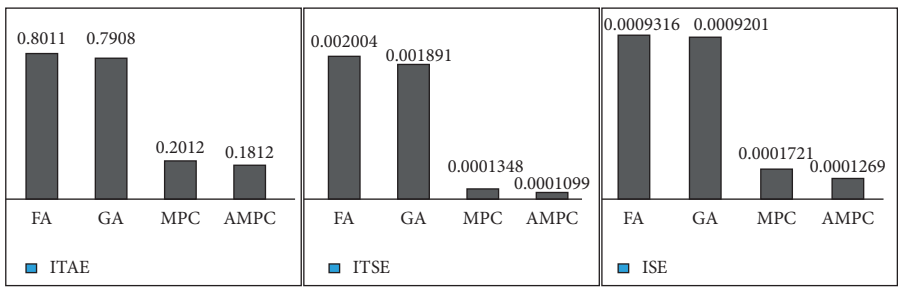

Figure 19: ITAE, ITSE, and ISE-based controller performance.

and it can deteriorate the frequency from its nominal value. Time delay usually occurs in the governor section as shown in Figure 16, and that for turbine is represented in Figure 17.

The stability response of the proposed controller is tested as shown in Figure 18.

If there is any uncertainty in the governing units of the thermal system, this might lead to a sudden breakdown of the overall system. To validate the effectiveness of the proposed controller, an uncertainty test is carried out where the proposed controller validates its robustness. The validation of the proposed technique can be verified by their performance indices; in this research work, three commonly used performance indices are presented: integral time absolute error (ITAE), integral time square error (ITSE), and integral square error (ISE), to verify the performance of the controllers. Table 1 defines the performance indices of different controllers.

The obtained performances of the controllers are analyzed in bar chart format to get a better idea. Figure 19 presents the ITAE, ITSE, and ISE-based controller performances.

6. Conclusion

(i) This paper has presented a control strategy for a hybrid thermal power system in which the fluctuation in frequency is controlled by a newly adaptive-based MPC controller. The two-area system is presented which is connected via a tie line. Modeling of PV and wind farms is presented where the impact of renewable sources is visualized.

(ii) The wind turbine system is controlled by MPC while the thermal section is controlled by AMPC to mitigate the effect of frequency fluctuation under load disturbance.

(iii) The AMPC deals with two main controlling components: initially, it deals with LFC requirements and later it deals with attenuation effect due to external disturbance to achieve zero tracking for tie line variation in frequency.

(iv) The overall proposed controlling mechanism quite effectively adapts to the unpredictable situation in the power system. Moreover, simulation results are presented under step, practical scenarios, and under uncertainty in the thermal power system which has shown the superiority of the proposed technique.

Data Availability

No data were used to support this study.

Conflicts of Interest

The authors declare that they have no conflicts of interest.

References

[1] D. Abu, Q. A. Ahmad, and H. Ahmad, "Stability analysis of connected large-scale renewable energy sources into Jordanian national power grid," *International Journal of Ambient Energy*, vol. 41, pp. 1–10, 2018.

[2] R. Adib, H. E. Murdock, F. Appavou et al., "Renewables 2015 global status report," REN21 Secretariat 83, Paris, France, 2015.

[3] T. Adefarati and R. C. Bansal, "Reliability and economic assessment of a microgrid power system with the integration of renewable energy resources," *Applied Energy*, vol. 206, pp. 911–933, 2017.

[4] W. Li, H. Ren, P. Chen, Y. Wang, and H. Qi, "Key operational issues on the integration of large-scale solar power generation-A literature review," *Energies*, vol. 13, no. 22, Article ID 5951, 2020.

[5] R. Shankar, S. R. Pradhan, K. Chatterjee, and R. Mandal, "A comprehensive state of the art literature survey on LFC mechanism for power system," *Renewable and Sustainable Energy Reviews*, vol. 76, pp. 1185–1207, 2017.

[6] M. M. Gulzar, D. Sibtain, A. F. Murtaza, S. Murawwat, M. Saadi, and A. Jameel, "Adaptive fuzzy based optimized proportional-integral controller to mitigate the frequency oscillation of multi-area photovoltaic thermal system," *International Transactions on Electrical Energy Systems*, vol. 31, Article ID e.12643, 2020.

[7] M. Hanan, X. Ai, M. Y. Javed, M. Majid Gulzar, and S. Ahmad, "A two-stage algorithm to harvest maximum power from photovoltaic system," in *Proceedings of the 2nd IEEE Conference on Energy Internet and Energy System Integration (EI2)*, pp. 1–6, Beijing, China, October 2018.

[8] S. M. Malik, X. Ai, Y. Sun, C. Zhengqi, and Z. Shupeng, "Voltage and frequency control strategies of hybrid AC/DC microgrid: a review," *IET Generation, Transmission & Distribution*, vol. 11, no. 2, pp. 303–313, 2017.

[9] W. Tan and R. Zhou, "Anti-windup schemes for load frequency control of power systems with governor deadband," in *Proceedings of the 12th IEEE Conference on Industrial Electronics and Applications (ICIEA)*, pp. 780–785, Siem Reap, Cambodia, June 2017.

[10] T. Banki, F. Faghihi, and S. Soleymani, "Frequency control of an island microgrid using reset control method in the presence of renewable sources and parametric uncertainty," *Systems Science & Control Engineering*, vol. 8, no. 1, pp. 500–507, 2020.

[11] M. Gulzar, S. Rizvi, M. Javed, D. Sibtain, and R. Salah ud Din, "Mitigating the load frequency fluctuations of interconnected power systems using model predictive controller," *Electronics*, vol. 8, no. 2, p. 156, 2019.

[12] A. Singh and S. Suhag, "Frequency regulation in an AC microgrid interconnected with thermal system employing multiverse-optimised fractional order-PID controller," *International Journal of Sustainable Energy*, vol. 39, no. 3, pp. 250–262, 2020.

[13] A. Dutta and S. Prakash, "Load frequency control of multi-area hybrid power system integrated with renewable energy sources utilizing FACTS & energy storage system," *Environmental Progress & Sustainable Energy*, vol. 39, no. 2, Article ID e13329, 2020.

[14] S. Daud, A. F. Murtaza, N. Ahmed, H. Ahmed Sher, and M. M. Gulzar, "Multi control adaptive fractional order PID control approach for PV/wind connected grid system," *International Transactions of Electrical Energy System*, vol. 31, pp. 1–21, Article ID e12809, 2021.

[15] M. Xie, M. M. Gulzar, H. Tehreem, M. Y. Javed, and S. T. H. Rizvi, "Automatic voltage regulation of grid connected photovoltaic system using lyapunov based sliding

mode controller: a finite—time approach," *International Journal of Control, Automation and Systems*, vol. 18, no. 6, pp. 1550–1560, 2020.

[16] H. Alhelou, M.-E. Hamedani-Golshan, R. Zamani, E. Heydarian-Forushani, and P. Siano, "Challenges and opportunities of load frequency control in conventional, modern and future smart power systems: a comprehensive review," *Energies*, vol. 11, no. 10, Article ID 2497, 10 pages, 2018.

[17] U. Khan, M. Majid Gulzar, S. Daud, H. Muhammad Usman, and A. Hayat, "Variable step size fractional incremental conductance for MPPT under changing atmospheric conditions," *International Journal of Numerical Modelling: Electronic Networks, Devices and Fields*, vol. 33, no. 6, Article ID e2765, 2020.

[18] V. P. Singh, P. Samuel, and N. Kishor, "Impact of demand response for frequency regulation in two-area thermal power system," *International Transactions on Electrical Energy Systems*, vol. 27, no. 2, Article ID e2246, 2017.

[19] Ö. Çelik and T. Ahmet, "A Hybrid MPPT method for grid connected photovoltaic systems under rapidly changing atmospheric conditions," *Electric Power Systems Research*, vol. 152, pp. 194–210, 2017.

[20] M. Sharma, S. Dhundhara, Y. Arya, and S. Prakash, "Frequency stabilization in deregulated energy system using coordinated operation of fuzzy controller and redox flow battery," *International Journal of Energy Research*, vol. 45, no. 5, pp. 7457–7475, 2021.

[21] Y. Arya, P. Dahiya, E. Çelik, G. Sharma, H. Gözde, and I. Nasiruddin, "AGC performance amelioration in multi-area interconnected thermal and thermal-hydro-gas power systems using a novel controller," *Engineering Science and Technology, an International Journal*, vol. 24, no. 2, pp. 384–396, 2021.

[22] A. M. Hemeida, "Wavelet neural network load frequency controller," *Energy Conversion and Management*, vol. 46, no. 9-10, pp. 1613–1630, 2005.

[23] K. S. Simhadri and B. Mohanty, "Performance analysis of dual-mode PI controller using quasi-oppositional whale optimization algorithm for load frequency control," *International Transactions on Electrical Energy Systems*, vol. 30, Article ID e12159, 2019.

[24] M. Z. Bernard, T. H. Mohamed, R. Ali, Y. Mitani, and Y. Soliman Qudaih, "PI-MPC frequency control of power system in the presence of DFIG wind turbines," *Engineering*, vol. 5, no. 9, p. 43, 2013.

[25] E. Çelik, N. Öztürk, Y. Arya, and C. Ocak, "(1 + PD)-PID cascade controller design for performance betterment of load frequency control in diverse electric power systems," *Neural Computing & Applications*, vol. 33, no. 22, pp. 15433–15456, 2021.

[26] Y. Arya, N. Kumar, P. Dahiya et al., "Cascade-$I\lambda D\mu N$ controller design for AGC of thermal and hydro-thermal power systems integrated with renewable energy sources," *IET Renewable Power Generation*, vol. 15, no. 3, pp. 504–520, 2021.

[27] K. Soleimani and J. Mazloum, "Designing a GA-based robust controller for load frequency control (LFC)," *Engineering, Technology & Applied Science Research*, vol. 8, no. 2, pp. 2633–2639, 2018.

[28] S. Aziz, H. Wang, Y. Liu, J. Peng, and H. Jiang, "Variable universe fuzzy logic-based hybrid LFC control with real-time implementation," *IEEE Access*, vol. 7, pp. 25535–25546, 2019.

[29] Z. Esfahani, M. Roohi, M. Gheisarnejad, T. Dragičević, and M.-H. Khooban, "Optimal non-integer sliding mode control for frequency regulation in stand-alone modern power grids," *Applied Sciences*, vol. 9, no. 16, Article ID 3411, 16 pages, 2019.

[30] G. Sharma, N. Krishnan, Y. Arya, and A. Panwar, "Impact of ultracapacitor and redox flow battery with JAYA optimization for frequency stabilization in linked photovoltaic-thermal system," *International Transactions on Electrical Energy Systems*, vol. 31, no. 5, Article ID e12883, 2021.

[31] H. Li, X. Wang, and J. Xiao, "Adaptive event-triggered load frequency control for interconnected microgrids by observer-based sliding mode control," *IEEE Access*, vol. 7, pp. 68271–68280, 2019.

[32] X. Zhao, J. He, B. Fu, L. He, and G. Xu, "A system compensation based model predictive AGC method for multiarea interconnected power systems with high penetration of PV system and random time delay between different areas," *Mathematical Problems in Engineering*, vol. 2018, Article ID 9347878, 10 pages, 2018.

[33] A. M. Othman and A. A. El-Fergany, "Design of robust model predictive controllers for frequency and voltage loops of interconnected power systems including wind farm and energy storage system," *IET Generation, Transmission & Distribution*, vol. 12, no. 19, pp. 4276–4283, 2018.

[34] J. Liu, Q. Yao, and Y. Hu, "Model predictive control for load frequency of hybrid power system with wind power and thermal power," *Energy*, vol. 172, pp. 555–565, 2019.

[35] K. B. Sahay and M. Goel, "Grid integrated solar photovoltaic array power plant modeling and simulation," in *Proceedings of the International Conference and Utility Exhibition on Green Energy for Sustainable Development (ICUE)*, pp. 1–5, Phuket, Thailand, October 2018.

[36] H. Abouobaida, J. Antonio, and M. Cardoso, "Fault-tolerent control strategy for dc-dc converter in power wind conversion system," in *Proceedings of the International Conference on Electronics, Control, Optimization and Computer Science (ICECOCS)*, pp. 1–6, Kenitra, Morocco, December 2018.

[37] G. Magdy, E. A. Mohamed, and G. Shabib, A. A. Elbaset and Y. Mitani, "Enhancement LFC of a realistic multi-source power system concerning wind farms using SMES and new optimized PID controller," in *Proceedings of the 2018 5th International Conference on Electric Power and Energy Conversion Systems (EPECS)*, pp. 1–7, Kitakyushu, Japan, April 2018.

[38] A. Murdoch, J. R. Winkelman, S. H. Javid, and R. S. Barton, "Control design and performance analysis of a 6 MW wind turbine-generator," *IEEE Power Engineering Review*, vol. PER-3, no. 5, p. 49, 1983.

[39] N. W. Miller, W. W. Price, and J. J. Sanchez-Gasca, "Dynamic modeling of GE 1.5 and 3.6 wind turbine-generators," in *Proceedings of the GE-Power Systems Energy Consulting*, Toronto, ON, Canada, July 2003.

[40] H. Bevrani, M. R. Feizi, and S. Ataee, "Robust frequency control in an islanded microgrid: and synthesis approaches," *IEEE H∞μ transactions on smart grid*, vol. 7, no. 2, pp. 706–717, 2016.

[41] J. Richalet, A. Rault, J. L. Testud, and J. Papon, "Model predictive heuristic control," *Automatica*, vol. 14, no. 5, pp. 413–428, 1978.

[42] J. B. Rawlings and D. Q. Mayne, *Model Predictive Control: Theory and Design*, Nob Hill Publishing, LLC, Madison, WI, USA, 2009.